Electrochemical Oxidation of 1,2-Dihydroxybenzene in Isoleucine Presence: Mechanistic Insights and Kinetic Evaluation

Firoz Ahmed[1], M. Abdul Motin[1*], M. A. Hafiz Mia[1] and M. A. Aziz[2]

[1]*Department of Chemistry, Khulna University of Engineering & Technology (KUET), Khulna, Bangladesh*

[2]*University of Global Village (UGV), Barishal, Bangladesh*

*Corresponding author: motin@chem.kuet.ac.bd

Received 24/06/2025; accepted 10/11/2025
https://doi.org/10.4152/pea.2027450510

Abstract

Electrooxidation behavior of 1,2-dihydroxybenzene (catechol) in the presence of isoleucine was systematically investigated in aqueous buffer solutions, over a pH range from 5 to 11, using cyclic voltammetry, differential pulse voltammetry, controlled-potential coulometry and Fourier transform infra-red spectroscopy. At higher concentrations of isoleucine, a secondary electrochemical response was observed during reverse scan, attributed to the formation of a product resulting from the reaction between *o*-benzoquinone and isoleucine. This product is (2S,3S)-2-((3,4-dihydroxyphenyl)amino)-3-methylpentanoic acid, which undergoes oxidation at more negative potentials than catechol. Electrochemical response was strongly influenced by both pH and isoleucine concentration, with optimal conditions identified at 70 mM isoleucine and 2 mM catechol in a buffer solution of pH 7. Overall mechanism was found to follow an electron transfer–chemical reaction–electron transfer pathway, governed by a diffusion-controlled process. These findings provide insight into amino acid–quinone interactions, and have potential implications for understanding redox processes in biological and electrochemical systems.

Keywords: catechol-isoleucine adduct; controlled potential coulometry; electrosynthesis; oxidation reaction pathway; voltammetry techniques.

Introduction•

1,2-dihydroxybenzene (Catechol) is an essential chemical intermediate frequently used in numerous organic synthesis, which is extensively applied in industrial manufacturing. It serves as a key intermediate in the manufacture of pesticides, fragrances, dyes and pharmaceutical agents [1]. In addition to its synthetic importance, catechol is naturally abundant in various plant-derived substances and it is recognized for its strong antioxidant activity [2]. A distinguishing feature of catechol is its propensity for oxidation, due to its low oxidation potential and electron-rich aromatic structure [3]. Upon oxidation, catechol readily forms *o*-

•The abbreviations list is in page 517.

benzoquinone, an electron-deficient and highly reactive species that participates in numerous subsequent chemical transformations [4]. Electrochemical methods offer a powerful and controlled approach for generation of *o*-quinones, making them attractive for studying redox behavior and facilitating downstream reactions [5]. Several investigations have explored electrooxidation of catechol to *o*-quinone, particularly focusing on its reactivity and mechanistic role in various homogeneous and biomimetic processes. These studies highlight the potential of catechol derivatives in redox biology, material science and electrochemical synthesis.

Isoleucine, one of the nine essential amino acids required by humans, plays a crucial role in several physiological processes [6]. It supports wound healing, aids in detoxification of nitrogenous waste, stimulates immune function and promotes secretion of various hormones [7]. Additionally, isoleucine is involved in hemoglobin synthesis and helps regulate blood glucose and energy levels, particularly within muscle tissues where it is highly concentrated [8]. Since the human body cannot synthesize isoleucine, it must be obtained through dietary intake from sources such as meat, fish, eggs, cheese, seeds and nuts [9-10]. In microorganisms like bacteria, isoleucine is biosynthesized from pyruvate via leucine biosynthesis enzymes [11-12]. Due to its nucleophilic amine group and biological relevance, isoleucine can serve as a suitable reactant for forming functionalized derivatives through reactions with electrophilic intermediates such as o-quinones, generated from electrochemical oxidation of catechol.

Electrochemical oxidation of catechols has been investigated in presence of various nucleophiles, including amino acids like proline, aspartic acid, glutamine, sulfanilic acid, ethanol, 2-thiobarbituric acid, β-diketones, 4-hydroxy-6-methyl-2-pyrone, 2-thiouracil, dimedone, 4,7-dihydroxycoumarin, 4,5,7-trihydroxycoumarin, 4-hydroxy-6-bromocoumarin, 3-hydroxycoumarin, 4-hydroxy-6-methyl-α-pyrone, 4-hydroxy-6-methyl-2-pyridone and 4-hydroxycarbostyrile [14-29]. These studies have provided significant insight into the electrochemical behavior of catechols and their reactivity with diverse nucleophiles, leading to formation of functionalized derivatives. However, to the best of the authors' knowledge, no studies have been conducted on electrochemical oxidation of catechols in the presence of isoleucine. Isoleucine, an essential amino acid with a nucleophilic amine group, presents an interesting opportunity to explore its reactivity with catechols under electrochemical conditions. In this paper, electrochemical behavior of catechol in presence of isoleucine was investigated, examining reaction kinetics at three different electrode materials, with varying concentrations of isoleucine and different pH conditions. The objective was to explore electrochemical interaction of catechol with isoleucine to generate a functionalized product with implications for both chemical synthesis and biological processes.

Experimental

Catechol, isoleucine, acetic acid, sodium acetate, potassium chloride, sodium dihydrogen phosphate and disodium hydrogen phosphate were all of analytical grade and procured from E. Merck (Germany). All solutions were prepared using distilled water. Acetate and phosphate buffer solutions were prepared and adjusted to desired pH (5–11) using Henderson–Hasselbalch equation. Solutions containing catechol and catechol–isoleucine mixtures at varying concentrations were prepared in either buffer solutions, depending on target pH.

Glassy carbon electrodes (GCE) (3.0 mm diameter), platinum and gold disk electrodes (1.6 mm diameter), obtained from Bioanalytical Systems, Inc. were employed as working electrodes in voltammetric studies. A set of three carbon rods (6 mm diameter, 4 cm length) was used as working electrode in CPC. Prior to each measurement, electrode surfaces were polished with 0.05 μm alumina on a polishing pad, rinsed thoroughly with deionized water, and inspected to ensure a mirror-like finish. A platinum coil and Ag|AgCl (3 M KCl) (Bioanalytical Systems, Inc.) was used as auxiliary and reference electrodes, respectively. Electrochemical experiments were performed employing a μStat 8000 potentiostat/galvanostat (Metrohm/DropSens). Before each electrochemical run, the one-compartment cell was deaerated by bubbling nitrogen gas through the solution for several minutes.

Results and discussion

Electrochemical behaviour of catechol with isoleucine

Electrochemical response of catechol in absence and presence of isoleucine was investigated using cyclic voltammetry (CV), differential pulse voltammetry (DPV) and controlled potential coulometry (CPC). Fig. 1 (black line) illustrates CV of catechol (2.0 mM) recorded on a GCE (3 mm diameter) in PBS (pH 7.0), at a scan rate of 0.1 V/s^{-1}.

A well-defined anodic peak was observed at 0.46 V, corresponding to oxidation of catechol to *o*-benzoquinone, followed by cathodic peak at 0.10 V associated with reverse reduction process. In contrast, pure isoleucine (70 mM) exhibited no discernible redox activity within studied potential window (Fig. 1, blue line), confirming its electrochemical inertness under these conditions. Upon addition of isoleucine to catechol solution, notable changes were observed in voltammetric profile during the second scan (Fig. 1, red line). The CV revealed two anodic peaks at −0.06 (A_0) and 0.28 V (A_1), along with corresponding cathodic peaks at −0.27 (C_0) and 0.08 V (C_1), respectively. The emergence of A_0/C_0 redox couple, alongside a decrease in peak currents of A_1 and C_1 and a shift in their potentials, strongly suggests a chemical interaction between catechol and isoleucine.

This behavior can be rationalized by a nucleophilic addition reaction, wherein amino group of isoleucine attacks electrophilic *o*-benzoquinone intermediate, forming a catechol–isoleucine adduct. The formation of this adduct lowers effective concentration of free *o*-benzoquinone in diffusion layer, thereby

diminishing intensity of original catechol redox peaks (A_1/C_1) while simultaneously giving rise to new peaks (A_0/C_0) corresponding to redox activity of the adduct. Notably, during first potential cycle, anodic response of catechol in presence of isoleucine closely resembled that of pure catechol, indicating minimal interaction at this stage. However, in subsequent scans, a marked decrease in current intensities of A_1 and C_1 was observed (Fig. 1, red line), in contrast to unchanged behavior of catechol alone (Fig. 1, black line), further supporting the occurrence of a follow-up chemical reaction between *o*-benzoquinone and isoleucine.

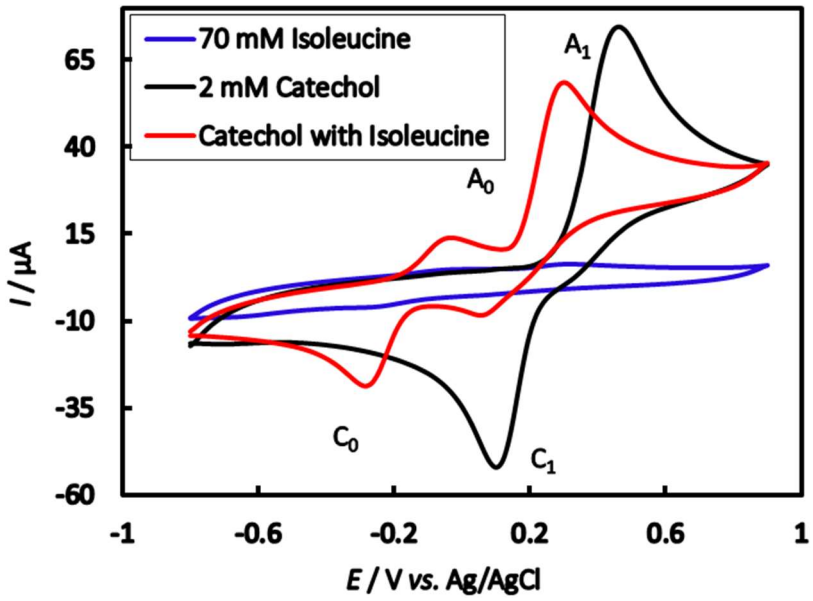

Figure 1: CV of catechol, isoleucine and 2 mM catechol with 70 mM isoleucine on GCE in PBS of pH 7, at scan rate of 0.1 V s^{-1} (2nd cycle). A0 and A1 are anodic peaks, and C0 and C1 are corresponding cathodic peaks

Ratio of anodic to cathodic peak currents for redox couple A_1/C_1 (I_{pa1}/I_{pc1}) exhibited a notable decrease with successive potential cycles, indicating occurrence of a follow-up chemical reaction between isoleucine and *o*-benzoquinone generated at the electrode surface (Step 1, Scheme 1). This observation supports the formation of a nucleophilic substitution product, identified as (2S,3S)-2-((3,4-dihydroxyphenyl)amino)-3-methylpentanoic acid (Step 2, Scheme 1). Such behavior is consistent with previous reports on electrochemical oxidation of catechols in presence of nucleophilic species such as proline, aspartic acid, glutamine and sulfanilic acid [13-16]. It has been established that when oxidation potential of the resultant product is sufficiently low, further oxidation is minimized, allowing for additional redox interactions and incorporation of other chemical functionalities [30].

In the present study, oxidation of isoleucine-substituted *o*-benzoquinone derivative (Step 3, Scheme 1) was found to proceed more readily than that of parent catechol. Although this intermediate could, in principle, undergo further nucleophilic attack

by isoleucine, such secondary reactions were not observed under applied voltammetric conditions, likely due to reduced electrophilicity of substituted quinone (compound 4). Eectrochemical formation of similar catechol–nucleophile adducts has been previously documented in systems involving various amino acids and aromatic amines [13–27]. In the absence of external nucleophiles, *o*-benzoquinone typically undergoes addition reactions with water or hydroxide ions present in aqueous media [30-31]. Reaction steps scheme is shown in Scheme 1.

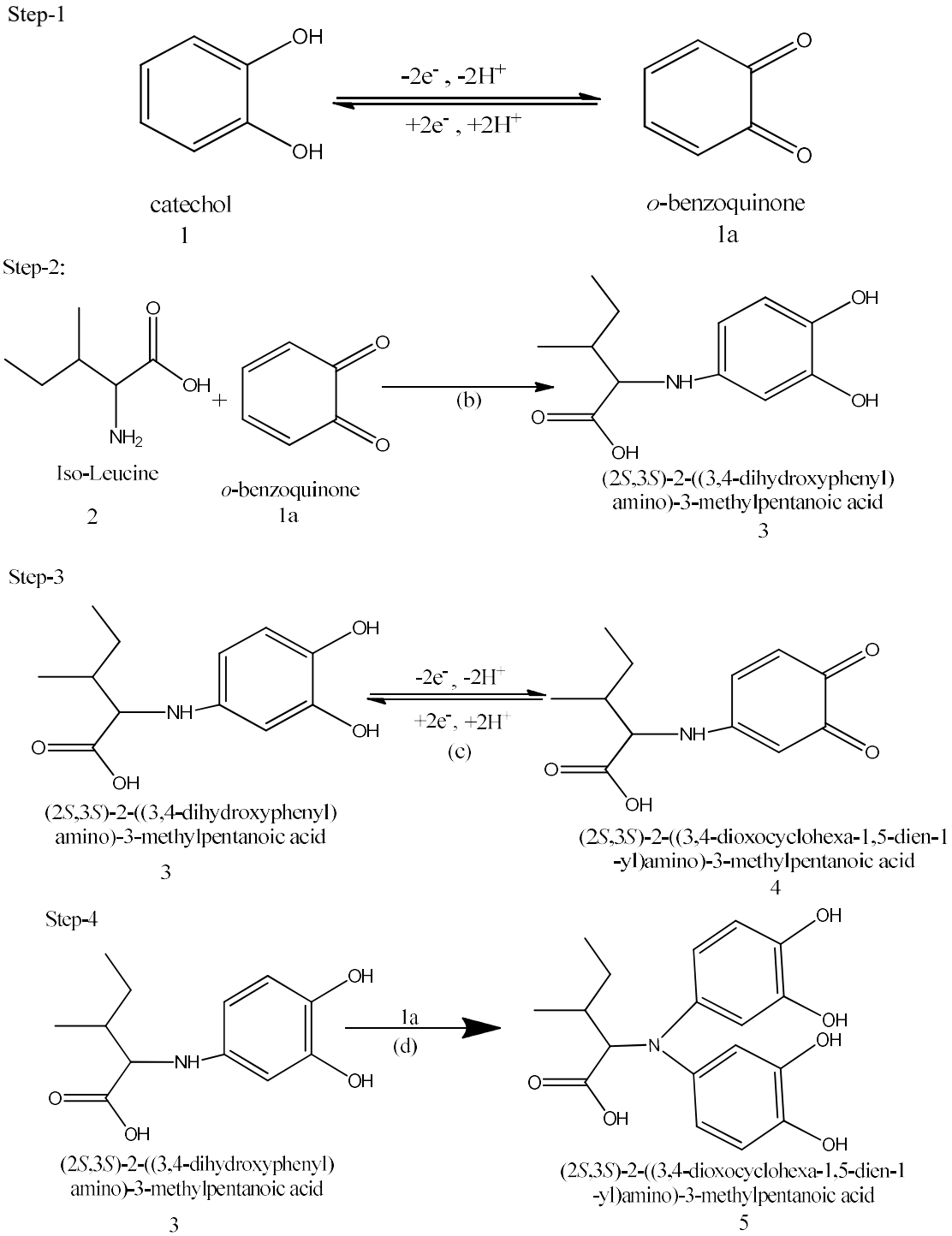

Scheme 1: Reaction steps of catechol oxidation in presence of isoleucine.

Scan rate studies and mechanistic insights

Fig. 2a presents CV of second cycle for catechol (2.0 mM) in presence of isoleucine (70 mM) at GCE (3 mm diameter) recorded at various scan rates in PBS (pH 7.0). As scan rate increased, both anodic and cathodic peak currents showed a corresponding increase, accompanied by a slight shift of redox peaks toward more negative potentials. Fig. 2b displays plots of net anodic and cathodic peak currents of A_1 and C_1 redox couples as a function of square root of scan rate. Net peak current was calculated using scan-stopped method, defined as the difference between second peak and the first [32]. Although peak currents exhibited a linear relationship with square root of scan rate, regression lines did not intersect the origin. This deviation implies that diffusion alone does not fully govern electron transfer process, and that a surface-confined or coupled chemical reaction likely contributes to overall behavior [33].

For A_0 and C_0 peaks, peak currents increased with square root of scan rate up to 0.5 V/s^{-1}. Anodic peak current ratio (I_{pa0}/I_{pa1}) for catechol–isoleucine system increased with growing scan rate up to 0.4 V/s^{-1}, after which it slightly declined (Fig. 2c).

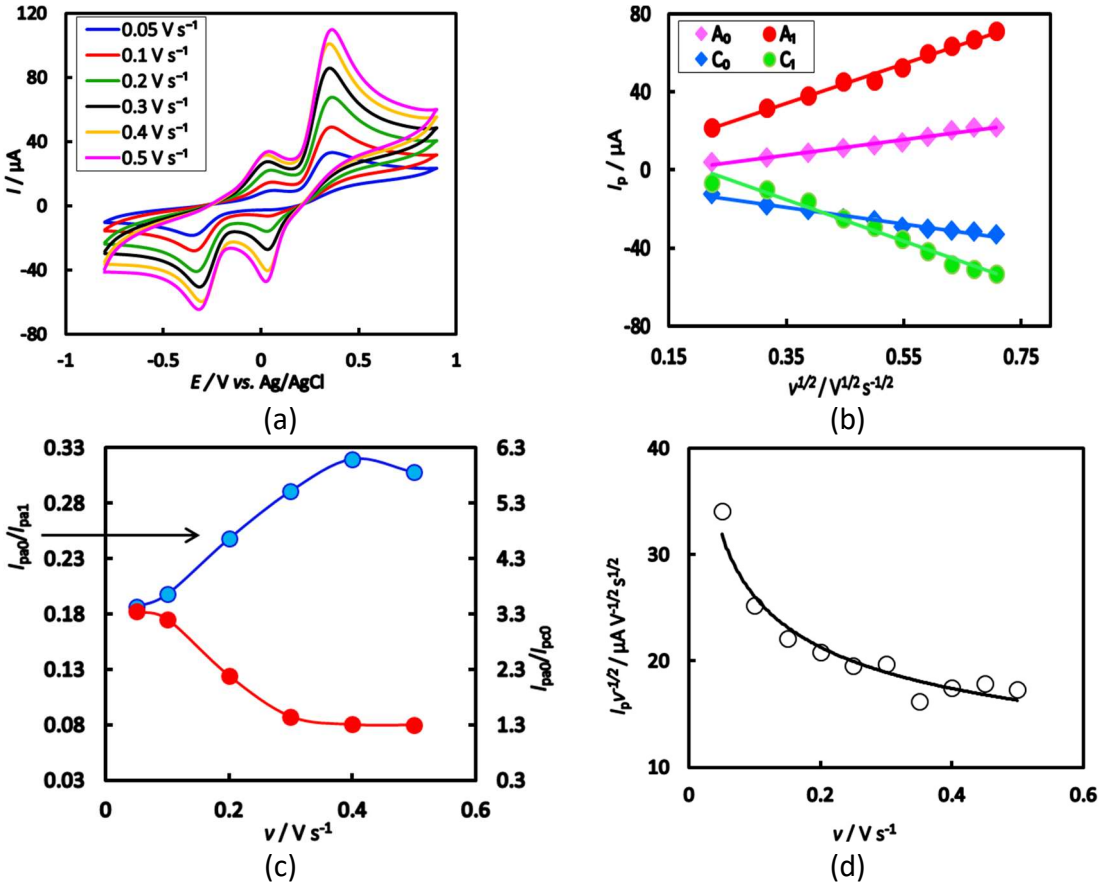

Figure 2: a) CV of 2 mM catechol with 150 mM isoleucine in second scan of potential at GCE in PBS of pH 7 at different scan rates; **b)** plots of peak current *vs.* square root of scan rate in same conditions. Legend shows symbols of oxidation and reduction peaks; **c)** variation of peak current ratio of corresponding peak (Ipa0/Ipc0) and anodic peak (Ipa0/Ipa1) *vs*. scan rate in same conditions; **d)** current function (Ip/v1/2) *vs.* scan rate.

Similarly, ratio of peak currents (I_{pa0}/I_{pc0}) decreased with increasing scan rate up to 0.3 V/s^{-1}, and then it stayed almost unchanged (Fig. 2c). Furthermore, current function ($I_p/v^{1/2}$) was found to decrease exponentially with increasing scan rate (Fig. 2d), suggesting the involvement of a coupled chemical step. The observed trend is consistent with an ECE (electrochemical–chemical–electrochemical) mechanism [17-18, 30], wherein an initial electron transfer is followed by a chemical reaction, which in turn is succeeded by a subsequent electron transfer step. This behavior implies that reactivity of *o*-benzoquinone (1a in Scheme 1) with isoleucine (2 in Scheme 1) is favored at lower scan rates, while it diminishes at higher scan rates, due to limited time for chemical interaction during potential sweep.

Evidence supporting occurrence of a subsequent chemical reaction between *o*-benzoquinone (1a) and isoleucine (2) is summarized as follows: in presence of isoleucine, both anodic (I_{pa1}) and cathodic (I_{pc1}) peak currents decrease during second potential cycle (see Fig. 1), indicating partial consumption of electrochemically generated *o*-benzoquinone through a chemical reaction with isoleucine; peak current ratio (I_{pa0}/I_{pc0}) decreases with increasing scan rate up to 0.3 V/s^{-1}, beyond which it remains relatively constant, which suggests that, at lower scan rates, a greater accumulation of cathodic species occurs due to longer reaction times, whereas, at higher scan rates, anodic species dominate; peak current (I_{pa0}/I_{pa1}) ratio initially increases with scan rate and then decreases, which indicates that faster scan rates reduce extent of the chemical reaction between 1a and 2 during voltammetric cycle, thereby limiting adduct formation [26]; exponential decrease in current function ($I_p/v^{1/2}$) with increasing scan rate supports ECE-type mechanism involving sequential electron transfer and chemical transformation [13, 14].

Collectively, these results suggest that 1,4-Michael addition of isoleucine (2) to *o*-benzoquinone (1a) yields compound 3 (Scheme 1). Oxidation of this adduct (3) occurs more readily than oxidation of parent catechol (1), likely due to electron-donating nature of amine functionality introduced by isoleucine, which facilitates electron transfer. CV of pure catechol were recorded in PBS (pH 7) at varying scan rates. A linear relationship was observed between both anodic and cathodic peak currents and square root of scan rate, indicating that redox process is predominantly diffusion-controlled under examined conditions.

Influence of pH

Electrochemical behavior of catechol was systematically studied in absence and presence of isoleucine over a pH range of 5 to 11 using CV. Experiments were performed with 2 mM catechol at a scan rate of 0.1 V/s^{-1} to evaluate the influence of the solution's pH on the electrode response. In absence of isoleucine, catechol exhibited a well-defined quasi-reversible redox couple at pH 7, with anodic peak potential shifting negatively as pH increased. This pH-dependent shift in potential

is consistent with a two-electron, two-proton redox process, as illustrated in Scheme 1 and previously reported in literature [34, 35].
In presence of 70 mM isoleucine, CV of catechol were recorded at a 3 mm GCE across the same pH range (Fig. 3a).

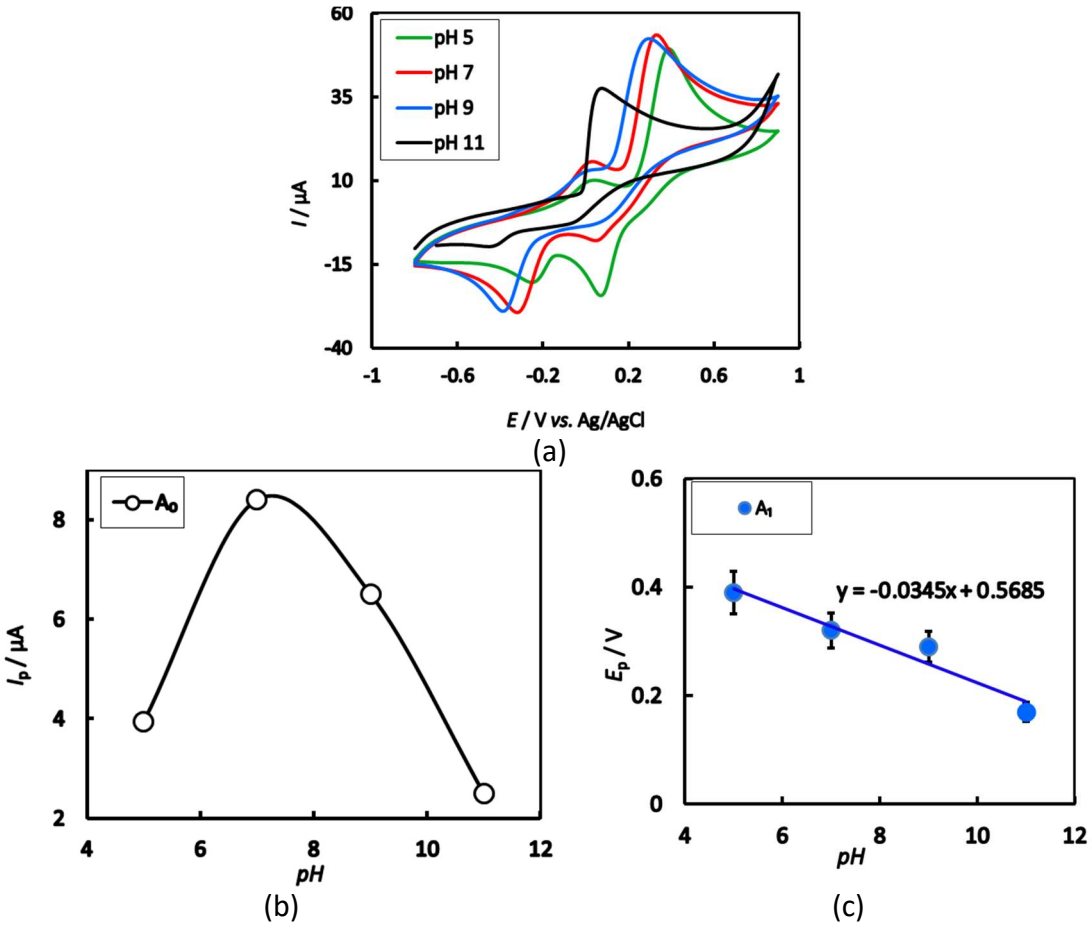

Figure 3: a) CV of 2 mM catechol with 70 mM isoleucine of GC (3 mm) electrode in buffer solutions of different pH, at a scan rate of 0.1 V s-1; **b)** plots of peak potential vs. pH in the same conditions; **c)** plots of peak current vs. pH in the same conditions. The meaning of symbols A0 and A1 is like in Fig. 1.

At pH 5–9, voltammograms revealed the development of new redox peaks during second scan, indicating formation of a catechol-isoleucine adduct via chemical interaction between o-benzoquinone and isoleucine. Notably, peak currents of newly formed anodic (A_0) and cathodic (C_0) signals were highest at pH 7 compared to pH 5 or 9, suggesting enhanced reactivity at neutral pH. In contrast, at higher pH values (pH 11), CV displayed irreversible electrochemical behavior. Under basic conditions, hydroxide ions, being stronger nucleophiles than isoleucine, rapidly react with electrochemically generated o-benzoquinone via a homogeneous chemical process. This reaction proceeds at a rate too fast to be captured on timescale of CV, thereby preventing observation of catechol-isoleucine interaction

[35]. These findings imply that, in alkaline media, catechol oxidation primarily involves irreversible reactions with hydroxide ions.

At neutral pH, reaction of o-benzoquinone with amine group of isoleucine proceeds via 1,4-Michael addition mechanism, resulting in appearance of new anodic peaks during voltammetric cycling. Fig. 3b shows dependence of anodic peak current (I_p) for A_0 on the solution's pH. Peak current was maximized at pH 7, further supporting the conclusion that neutral conditions favor formation and subsequent oxidation of catechol-isoleucine adduct. Additionally, peak current ratio (I_{pa_0}/I_{pc_1}) exhibited the greatest difference between presence and absence of isoleucine at pH 7. This suggests that electrochemical oxidation of catechol in presence of isoleucine is most efficient under neutral conditions, likely due to enhanced electron transfer kinetics. Therefore, PBS of pH 7 was selected as optimal medium for subsequent electrochemical investigations of catechol-isoleucine system.

Peak positions of redox couples were observed to vary with pH. Fig. 3c presents plot of oxidation peak potential (E_p) versus pH for anodic peaks A_0 and A_1. Slope of plot for A_1 was determined to be 34.5 mV/pH, which closely aligns with theoretical Nernstian value expected for a two-proton, two-electron process. This observation confirms that both catechol and catechol-isoleucine adduct undergo electrochemical oxidation via $2e^-/2H^+$ mechanism, consistent with pathway proposed in Scheme 1. Data also imply that both protons and electrons are released from catechol-isoleucine intermediate during redox process. Similar behavior has been reported for catechol and structurally related compounds [16-18, 26, 36].

Concentration effect of isoleucine

Influence of isoleucine concentration on electrochemical behavior of catechol was investigated by recording CV with increasing concentrations of isoleucine (50, 70, 100 and 150 mM) at a fixed catechol concentration (2 mM), using a 3 mm GCE in PBS (pH 7), at a scan rate of 0.1 V/s^{-1} (Fig. 4a).

As concentration of isoleucine increased from 50 to 70 mM, net current of newly emerging anodic (A_0) and cathodic (C_0) peaks increased, indicating enhanced formation of catechol-isoleucine adduct via nucleophilic substitution. However, further increases in isoleucine concentration beyond 70 mM resulted in a decrease in peak current intensity for both anodic and cathodic responses (Fig. 4b). This decline may be attributed to accumulation of excess electrochemically inactive isoleucine on the electrode surface, which could hinder electron transfer by partially blocking active sites. These results suggest that electrochemical reaction between catechol and isoleucine is most efficient at an isoleucine concentration of 70 mM under neutral pH conditions. Therefore, 70 mM isoleucine was considered optimal concentration for subsequent studies involving catechol-isoleucine interactions.

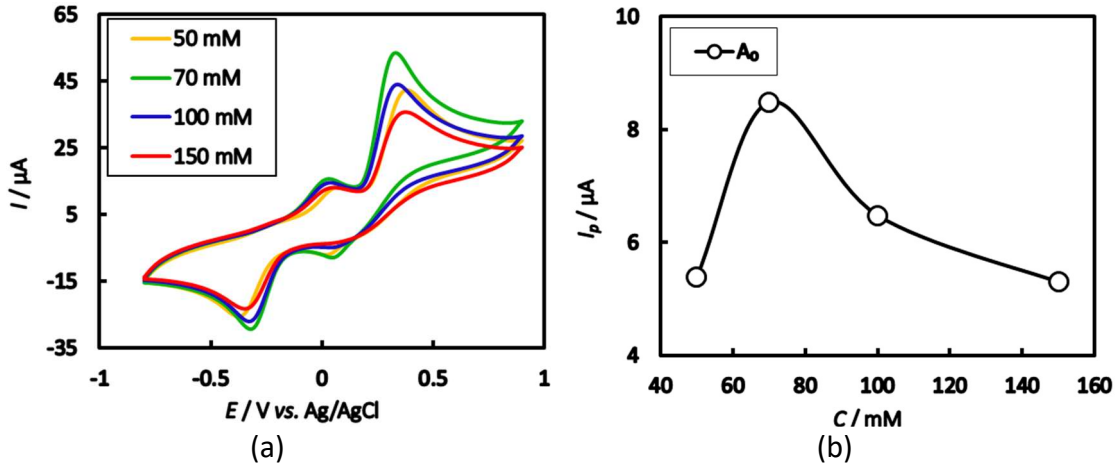

(a) (b)

Figure 4: **a)** CV of composition changes of isoleucine with fixed 2 mM catechol at GCE in buffer solution at pH 7,and scan rate 0.1 V s-1; **b)** plots of anodic peak current *vs.* concentration of isoleucine with fixed 2 mM catechol in the same conditions.

Effect of electrode materials

Electrochemical behavior of catechol, both in absence and presence of isoleucine, was evaluated using different electrode materials, including glassy carbon, gold (Au) and platinum (Pt), under varying pH conditions. Fig. 5a presents CV of 2 mM catechol in presence of 70 mM isoleucine recorded at GC, Au and Pt electrodes in phosphate buffer (pH 7), at a scan rate of 0.1 V/s^{-1}. Despite the larger diameter of GCE compared to Au and Pt electrodes, notable differences in voltammetric characteristics—such as peak positions and current intensities—were observed across the various electrode materials. In second potential cycle, all three electrodes exhibited emergence of new anodic and cathodic peaks at lower oxidation potentials, which are attributed to electrochemical response of the adduct formed between electrochemically generated o-benzoquinone and isoleucine. Specifically, GC, Au and Pt electrodes exhibited two well-defined redox couples corresponding to catechol-isoleucine adducts at approximately 0.05/-0.34, -0.06/-0.27 and -0.06/-0.27 V, respectively.

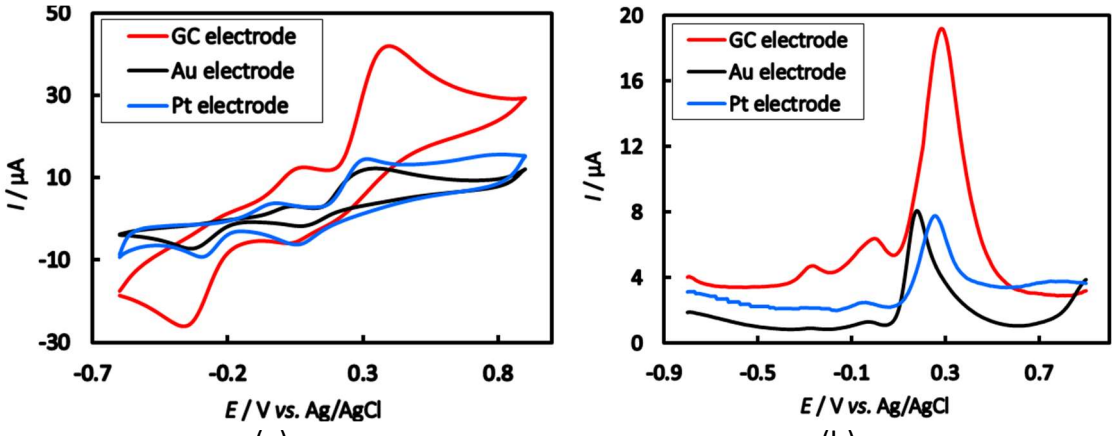

(a) (b)

Figure 5: a) CV and b) DPV of 2 mM catechol with 150 mM isoleucine at GCE, gold and platinum electrodes in a buffer solution of pH 7, at scan rate of 0.1 V/s-1

DPV experiments conducted under the same conditions (Fig. 5b) showed similar trends, with consistent adduct-related peak responses across all electrodes. However, three peaks appeared at GCE, which has demonstrated superior electrochemical performance in terms of peak definition, current intensity and resolution. Due to its favorable characteristics, GCE was selected for subsequent studies focused on electrochemical analysis of catechol in presence of isoleucine.

Subsequent cycles of CV from catechol-isoleucine derivative

Fig. 6a presents C from 2 mM catechol in presence of 70 mM isoleucine over initial 15 consecutive potential cycles using a 3.0 mm GCE in PBS (pH 7), within a potential window from -0.8 to 0.9 V and at a scan rate of 0.1 V/s^{-1}. In the first cycle, a distinct anodic peak appeared at 0.27 V, with a corresponding cathodic peak at -0.29 V (red line). In subsequent scans, a new anodic peak emerged near 0.01 V, while current of original anodic peak (A_0) progressively increased. Conversely, newly developed anodic peak current gradually decreased and shifted toward more positive potentials with continued cycling.

This evolving voltammetric behavior is attributed to formation of a catechol-isoleucine adduct via nucleophilic substitution reaction with electrochemically generated o-benzoquinone at the electrode surface (see Scheme 1). Increasing formation of this adduct led to a reduction in available concentration of free catechol and o-benzoquinone at the electrode interface, resulting in a gradual decline in redox peak intensity associated with catechol. Notably, during first ten cycles, anodic peak current of the newly formed adduct increased but later stabilized, likely due to surface passivation by accumulated electro-inactive species blocking active sites on GCE.

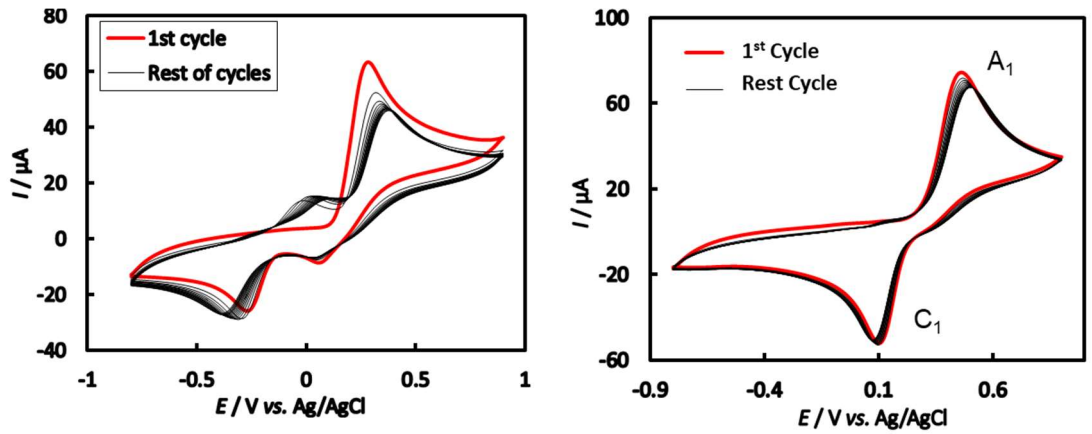

Figure 6: a) CV of 70 mM isoleucine with 2mM catechol on GC (3 mm) electrode in buffer solution of pH 7, at scan rate of 0.1 V s-1 (15 cycles). The first cycle is denoted by the red line and the other ones by black lines

Fig. 6b presents CV of 2 mM catechol recorded over first 15 cycles at GCE (3 mm) in a pH 7 PBS, using a scan rate of 0.1 V/s^{-1}. In the initial cycle (red line), a

single anodic peak is observed at 0.46 V, along with a corresponding cathodic peak at 0.09 V. No additional anodic peaks emerge in subsequent cycles, indicating that catechol undergoes a reversible redox process involving its conversion to o-benzoquinone, as depicted in Scheme 1. Nearly constant ratio of anodic to cathodic peak currents across cycles suggests electrochemical stability of o-benzoquinone product formed at the electrode surface. This observation implies that side reactions such as hydroxylation or dimerization occur at rates too slow to be detected within experimental timescale of CV [34, 37-38].

Upon addition of 70 mM isoleucine during the first cycle (Fig. 6a), cathodic peak shifts, which is attributed to a decrease in concentration of free catechol species due to its interaction with isoleucine. No new reduction peak is observed. However, in the second scan, a new anodic peak emerges at approximately -0.01 V, which is ascribed to oxidation of an adduct formed between o-benzoquinone and isoleucine, consistent with the proposed mechanism shown in Scheme 1. Anodic (A0) and cathodic (C0) peak currents increased with iteration scan from the first cycle. CPC was carried out in an aqueous PBS (pH 7) containing 1 mM catechol and 35 mM isoleucine at an applied potential of 0.5 V. Pogress of electrolysis was monitored at 30-min intervals using CV and DPV, as illustrated in Fig. 7.

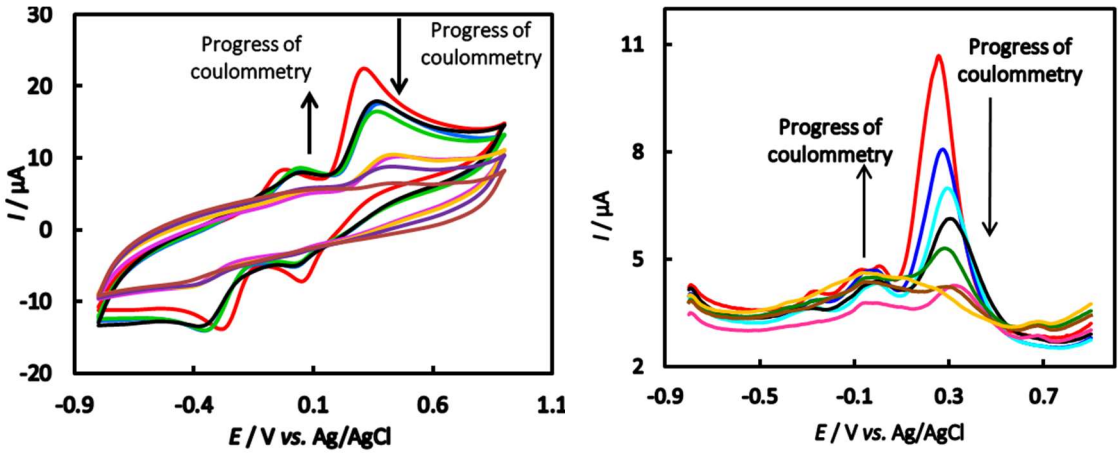

Figure 7: a) CV and **b)** DPV (taken after a 30-min interval) of 1 mM catechol in presence of 35 mM isoleucine on GCE in buffer solution of pH 7 during controlled potential coulometry at 0.5 V and scan rate of 0.1 V/s-1

At the beginning of electrolysis, distinct anodic and cathodic peaks, denoted as A_0 and C_0, were observed, which, with prolonged electrolysis, gradually diminished and eventually disappeared. Simultaneously, a progressive decrease in peak currents corresponding to A_1 and C_1 was also observed, as shown in Fig. 1. These results suggest consumption of catechol and its reaction products over electrolysis course.

Eventually, upon passage of approximately four electrons per molecule of catechol, all characteristic anodic and cathodic peaks disappeared, indicating

complete consumption of electroactive species. These findings support mechanistic pathway proposed in Scheme 1 for electrochemical oxidation of catechol (1) in presence of isoleucine (2). Specifically, data suggest that 1,4-Michael addition of isoleucine to electrochemically generated rapidly proceeding o-benzoquinone (1a), yielding intermediate 3. Oxidation of this intermediate is thermodynamically more favorable than that of parent catechol molecule, due to the electron-donating nature of amine substituent introduced through nucleophilic attack. Furthermore, data indicate potential for a second nucleophilic addition at C-5 position of a subsequent o-quinone derivative (4) by isoleucine. However, no significant secondary reactions were detected under employed voltammetric conditions. This lack of reactivity may be attributed to lower electrophilic character of quinone 4, rendering it less susceptible to further Michael-type addition reactions with isoleucine under experimental timescale.

Differential pulse voltammetry

Fig. 8 displays DPV recorded during second potential scan for 2 mM catechol in presence of 70 mM isoleucine across a range of buffer solutions with pH values from 5 to 11.

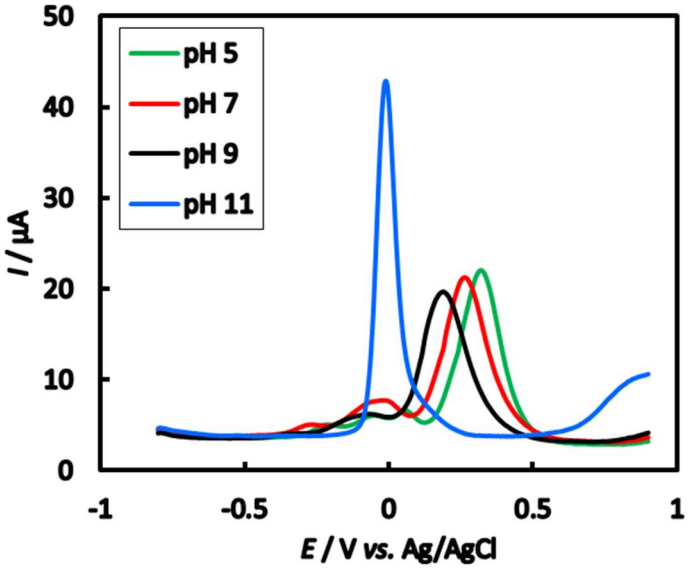

Figure 8: DPV in second scan of 2 mM catechol with 70 mM isoleucine of GCE at different pH levels of buffer solution and scan rate of 0.1 V/s-1

At pH 7, the voltammogram revealed three well-defined anodic peaks located at -0.24, 0.01 and 0.25 V, respectively. These peaks are attributed to stepwise oxidation of catechol and its reaction intermediate formed with isoleucine. Highest peak current intensities for A_0 were observed at pH 7, indicating optimal electrochemical reactivity under neutral conditions. In contrast, significantly lower peak currents were recorded at pH 5 and 9, suggesting diminished electrochemical response in acidic and alkaline media. At pH 11, anodic peak corresponding to A_1 was not observed, suggesting that, under alkaline conditions, catechol oxidation

proceeds predominantly through irreversible reactions with hydroxide ions. DPV results were found to be consistent with CV data presented earlier (Figs. 3 and 8), reinforcing pH-dependent behavior of catechol–isoleucine system. Enhanced anodic responses at pH 7 are likely due to efficient formation and subsequent oxidation of o-benzoquinone–isoleucine adduct (intermediate 3), as proposed in Scheme 1. Although intermediate 3 may undergo further nucleophilic attack by an additional isoleucine molecule, the resulting product was detected under DPV.

Effect of deposition time in DPV

Fig. 9 presents DPV responses recorded at various deposition times (0, 10, 30, 60, and 90 s) for a solution containing 2 mM catechol and 70 mM isoleucine in a pH 7 buffer. At 0 s, only a single anodic peak was observed at approximately 0.25 V. After 10 s deposition, two additional anodic peaks appeared at around -0.24 and 0.01 V. This observation suggests that increased deposition time facilitates nucleophilic substitution at the electrode interface, leading to enhanced formation of catechol–isoleucine adduct and concomitant decrease in concentration of free o-benzoquinone. Anodic peak current associated with the adduct reaches its maximum at deposition time of 30 s, indicating optimal accumulation of reactive intermediate at the electrode surface. However, further increases in deposition time to 60 and 90 s result in a marked decline in both anodic peak currents. This decrease may be attributed to saturation of the electrode surface by electro-inactive catechol–isoleucine product or to depletion of o-benzoquinone in the vicinity of the electrode. These results indicate that a deposition time of 30 s provides most favorable conditions for electrochemical detection of catechol–isoleucine adduct under studied conditions.

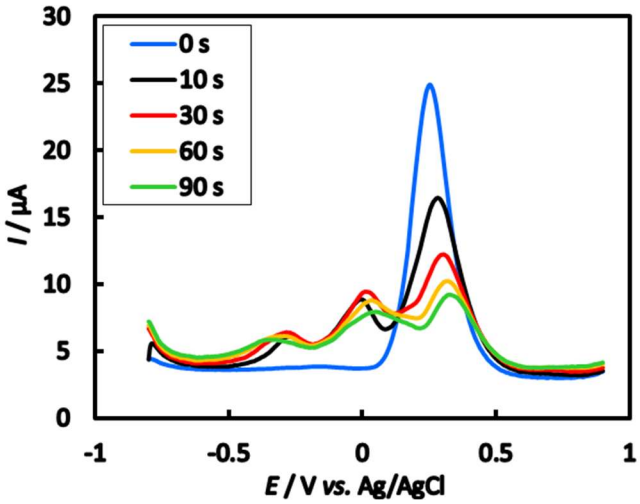

Figure 9: DPV of 2 mM catechol with 70 mM isoleucine in buffer solution of pH 7 for various deposition time changes at Epuls 0.02 V, tpuls 20 ms and scan of rate 0.1 V s-1

Influence of isoleucine concentration on electrochemical behavior of catechol was further investigated using DPV, as shown in Fig. 10. Measurements were

performed in a solution containing 2 mM catechol and varying concentrations of isoleucine (50-150 mM) in a pH 7 buffer. Consistent with CV results presented in Fig. 1, DPV responses revealed three distinct anodic peaks upon addition of isoleucine, corresponding to formation of electroactive adduct species. An increase in isoleucine concentration up to 70 mM led to a progressive enhancement in current of first anodic peak, indicating improved nucleophilic substitution of o-benzoquinone by isoleucine at the electrode surface. However, further increases in isoleucine concentration (100-150 mM) resulted in a gradual decrease in current intensity of all anodic peaks. This reduction is likely due to accumulation of excess electroinactive isoleucine on the electrode surface, which may hinder electron transfer processes and reduce availability of reactive catechol species. At lower concentrations (<60 mM), extent of nucleophilic substitution remained comparable, suggesting that optimal electrochemical reactivity is achieved near 70 mM isoleucine. Beyond this threshold, decline in peak current highlights the inhibitory effect of high isoleucine concentrations on the surface-confined redox process.

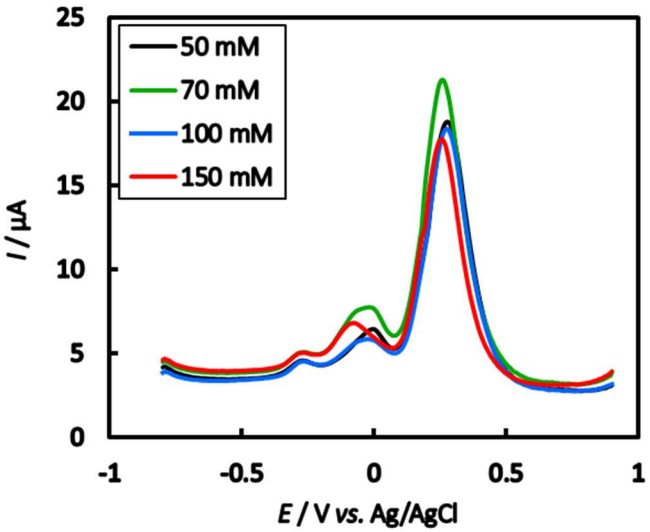

Figure 10: DPV of 2 mM catechol at different isoleucine concentrations in the second scan of pH 7 at Epuls 0.02 V, tpuls 20 ms of GCE and at a scan rate of 0.1 V/s

Spectral analysis of catechol with isoleucine

FTIR spectrum of catechol–isoleucine adduct was recorded in wavenumber range from 400 to 4000 cm^{-1} (Fig. 11). Pure catechol exhibited a characteristic O–H stretching band at 3385 cm^{-1}, while isoleucine displayed a broad absorption centered around 2960 cm^{-1}. In the spectrum of catechol–isoleucine adduct, broad O–H and N–H overlapping stretching vibration was observed at 3379 cm^{-1}. A noticeable decrease in intensity of the N–H stretching band was also evident, accompanied by significant changes in fingerprint region. These spectral alterations endorse the formation of a covalent adduct between catechol and

isoleucine via nucleophilic substitution. Similar spectral features have been reported in prior studies of catechol derivatives [13].

Collectively, these findings corroborate electrochemical results, indicating that nucleophilic substitution reaction between catechol and isoleucine proceeds most effectively at a concentration of 70 mM isoleucine and 2 mM catechol in a pH 7 buffer using a GCE. FTIR results are consistent with trends observed in CV and DPV, further validating the formation of catechol–isoleucine adduct under these conditions.

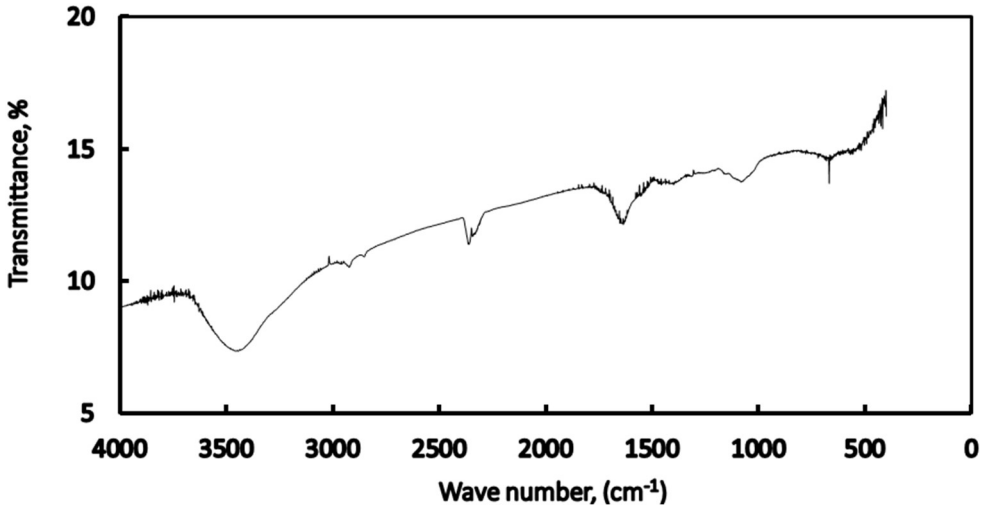

Figure 11: FTIR spectrum of catechol-isoleucine adduct.

Conclusions

Electrochemical behavior of catechol in absence and presence of isoleucine was systematically investigated using CV, DPV, CPC and FTIR spectroscopy. To determine optimal conditions for nucleophilic substitution reaction between catechol and isoleucine, effects of pH, electrode material,and analyte concentration were thoroughly examined. Upon electrochemical oxidation, catechol is converted to o-benzoquinone, which undergoes nucleophilic attack by isoleucine to form electroactive adducts. These adducts are further oxidized at more negative potentials than parent catechol. Oxidation of catechol–isoleucine adduct proceeds via a one-step $2e^-/2H^+$ process. Among tested electrode materials, GCE exhibited superior voltammetric performance compared to gold and platinum electrodes. Redox peak currents associated with catechol–isoleucine adducts were diffusion-controlled.

Nucleophilic addition reaction was most favorable at a concentration of 2 mM catechol and 70 mM isoleucine in a pH 7 buffer solution, utilizing a GCE. Electrochemical synthesis of catechol–isoleucine adduct during CPC analysis was further corroborated by FTIR spectroscopy. overall reaction mechanism follows ECE (electron transfer–chemical reaction–electron transfer) pathway, highlighting the interplay between electrochemical and chemical steps in the formation of catechol–isoleucine adduct.

Acknowledgments
The authors acknowledge the Ministry of Science and Technology, Government of the People's Republic of Bangladesh and KUET for providing necessary facilities and financial support to this research work.

Abbreviations
CPC: controlled potential coulometry
CV: cyclic voltammetry
DPV: differential pulse voltammetry
FTIR: Fourier transform infra-red spectroscopy
GCE: Glassy carbon electrode
PBS: phosphate buffer solution

Authors contributions
All authors contributed equally for the study and the paper writing.

References
1. Barner AB, Bongat AFG, Demchenko AV. "Catechol" in encyclopedia of reagents for organic synthesis. J Wiley & Sons, New York. 2004.
2. Khalafi L, Rafiee M. Kinetic study of the oxidation and nitration of catechols in the presence of nitrous acid ionization equilibria. J Hazardous Mater. 2010;174:801-806. https://doi.org/10.1016/j.jhazmat.2009.09.123
3. Bisby RH, Brooke R. Navaratnam S. Effect of antioxidant oxidation potential in the oxygen radical absorption capacity (ORAC) assay. Food Chem. 2008;108:1002-1007. https://doi.org/10.1016/j.foodchem.2007.12.012
4. Rafiee M. The electron: the simplest chemical reagent. Synlett. 2007;3:503-504. https://doi.org/10.1055/s-2006-967938
5. Nematollahi D, Rafiee M, Fotouhi L. Mechanistic study of homogeneous reactions coupled with electrochemical oxidation of catechols. J Iran Chem Soc. 2009;6:448-476. https://doi.org/10.1007/BF03246523
6. Wu, G. Functional Amino Acids in Growth, Reproduction, and Health. Adv Nutr. 2010;1(1);31-37. https://doi.org/10.3945/an.110.1008
7. Zhang S, Zeng X, Ren M et al. Novel Metabolic and Physiological Functions of Branched Chain Amino Acids: A Review. J Anim Sci Biotechnol. 2017;8:10. https://doi.org/10.1186/s40104-016-0139-z
8. Layman DK. The Role of Leucine in Weight Loss Diets and Glucose Homeostasis. J Nutr. 2003;133(1):261S-267S. https://doi.org/10.1093/jn/133.1.261S
9. Trumbo P, Schlicker S, Yates AA et al. Dietary reference intakes for energy, carbohydrate, fiber, fat, fatty acids, cholesterol, protein and amino acids. J Am Diet Assoc. 2002;102(11):1621-30. https://doi.org/10.1016/s0002-8223(02)90346-9
10. National Center for Biotechnology Information. PubChem Compound Summary for CID 6306, Isoleucine. https://pubchem.ncbi.nlm.nih.gov/compound/Isoleucine

11. Umbarger HE, Amino Acid Biosynthesis and Its Regulation. Ann Rev Biochem. 1978;47:533-606. http://dx.doi.org/10.1146/annurev.bi.47.070178.002533
12. Zinger B, Miller LL. Timed release of chemicals from polypyrrole films. J Am Chem Soc. 1984;106:6861-6863. https://doi.org/10.1021/ja00324a03.
13. Ahmed F, Motin MA, Hafiz Mia MA et al. Electrooxidation of catechol in the presence of proline at different pH. J Electrochem Sci Eng. 2025;15(2):2649. http://dx.doi.org/10.5599/jese.2649
14. Motin MA, Uddin MA, Dhar PK et al. Voltammetric electro-synthesis of catechol-aspartic acid adduct at different pHs and concentrations. Analyt Bioanalyt Electrochem. 2016;8:505-521.
15. Motin MA, Uddin MA, Uddin MN et al. Study of electrochemical oxidation of catechol in the presence of sulfanilic acid at different pH. Port Electrochim Acta. 2017;35:103-116. https://doi.org/10.4152/pea.201702103
16. Hafiz MA, Motin MA, Huque EM et al. Electro-oxidation of catechol in the presence of L-glutamine at different pH and concentrations. Analyt Bioanalyt Electrochem. 2017;9:597-613
17. Hafiz MA, Motin MA, Huque EM. Electrochemical Oxidation of Catechol in the Presence of L-Lysine at Different pH. Russ J Electrochem. 2019;55:370. https://doi.org/10.1134/S1023193519050070
18. Hafiz MA, Motin MA, Huque EM. Electrochemical Characterization of Catechol-Dimethylamine Adduct at Different pH Values. Port Electrochim Acta. 2018;36:437. https://doi.org/10.4152/pea.201806437
19. Hafiz MA, Motin MA, Huque EM. Electrooxidation of catechol in the presence of l-histidine at different Ph. Analyt Bioanalyt Electrochem. 2018;10:974.
20. L. Khalafi, M. Rafiee, M. Shahbak, H. Shirmohammadi. J Chem. 2013;2013:497515. https://doi.org/10.1155/2013/497515
21. Shahrokhian S, Hamzehloei A. Electrochemical oxidation of catechol in the presence of 2-thiouracil: application to electro-organic synthesis. Electrochem Commun. 2003;5:706-710. https://doi.org/10.1016/S1388-2481(03)00170-X
22. Nematollahi D, Golabi SM. Investigation of the electromethoxylation reaction Part 2: Electrochemical study of 3-methylcatechol and 2,3-dihydroxybenzaldehyde in methanol. Electroanalysis. 2001;13:1008. https://doi.org/10.1002/1521-4109(200108)13:12<1008::AID-ELAN1008>3.0.CO;2-1
23. Nematollahi D, Goodarzi H. Electrochemical study of catechol and some of 3-substituted catechols in the presence of 1,3-diethyl-2-thio-barbituric acid. Application to the electro-organic synthesis of new dispirothiopyrimidine derivatives. J Electroanalyt Chem. 2001;510:108-114. https://doi.org/10.1016/S0022-0728(01)00553-8

24. Tabakovic I, Grujic Z, Bejtovic Z. Electrochemical synthesis of heterocyclic compounds. XII. Anodic oxidation of catechol in the presence of nucleophiles. J Heterocyclic Chem. 1983;20:635-638. https://doi.org/10.1002/jhet.5570200325
25. Nematollahi D, Forooghi Z. Electrochemical oxidation of catechols in the presence of 4-hydroxy-6-methyl-2-pyrone. Tetrahedron. 2002;58:4949-4953. https://doi.org/10.1016/S0040-4020(02)00422-2
26. Golabi SM, Nourmohammadi F, Saadnia A. Electrochemical synthesis of organic compounds: 1. Addition of sulfinic acids to electrochemically generated o- and p-benzoquinones. J Electroanalyt Chem. 2002;529:12-19. https://doi.org/10.1016/S0022-0728(02)00906-3
27. Kiani A, Raoof JB, Nematollahi D et al. Electrochemical study of catechol in the presence of dibuthylamine and diethylamine in aqueous media: Part 1. Electrochemical investigation. Electroanalysis. 2005;17:1755-1760. https://doi.org/10.1002/elan.200503279
28. Janeiro P, Maria A, Brett O. Catechin electrochemical oxidation mechanisms. Analyt Chim Acta. 2004;518:109-115 https://doi.org/10.1016/j.aca.2004.05.038
29. Masek A, Chrzescijanska E, Zaborski M. Electrochemical Properties of Catechin in Non-Aqueous Media. Intern J Electrochem Sci. 2015;10:2504-2514. https://doi.org/10.1016/S1452-3981(23)04864-2
30. Papouchado L, Sandford RW, Petrie G et al. Anodic oxidation pathways of phenolic compounds Part 2. Stepwise electron transfers and coupled hydroxylations. J Electroanalyt Chem. 1975;65:275-284.
31. Thibodeau PA, Paquette B. DNA damage induced by catecholestrogens in the presence of copper (II): generation of reactive oxygen species and enhancement by NADH. Free Radic Biol Med. 1999;27:1367-1377. https://doi.org/10.1016/S0891-5849(99)00183-5
32. Bard AJ, Faulkner LR, Electrochemical Methods Fundamentals and Applications, Second Edition, John Wiley & Sons, 2001;226
33. Motin MA, Nishiumi T, Aoki KA. Symmetric redox reactions of C_3-symmetric starburst compound with six arylamines. J Electroanalyt Chem. 2007;601:139. https://doi.org/10.1016/j.jelechem.2006.11.002
34. Nematollahi D, Afkhami A, Mosaed F et al. Investigation of the electrooxidation and oxidation of catechol in the presence of sulfanilic acid. Res Chem Intermed. 2004;30:299-309. https://doi.org/10.1163/156856704323034030
35. Papouchado L, Petrie G, Adams RN. Anodic oxidation pathways of phenolic compounds: Part I. Anodic hydroxylation reactions. J Electroanalyt Chem. 1972;38:389-395. https://doi.org/10.1016/S0022-0728(72)80349-8
36. Papouchado L, Petrie G, Sharp JH et al. Anodic hydroxylation of aromatic compounds. J Am Chem Soc. 1968;90:5620-5621.

37. Rayn MD, Yueh A, Yu CW. The electrochemical oxidation of substituted catechols. J Electrochem Soc. 1980;127:1489-1495. https://doi.org/10.1149/1.2129936
38. Pasta M, Mantia FL, Cui Y. Mechanism of glucose electrochemical oxidation on gold surface. Electrochim Acta. 2010;55:5561-5568. https://doi.org/10.1016/j.electacta.2010.04.069